Journal of Nuclear Materials 377 (2008) 415–422

Contents lists available at ScienceDirect

Journal of Nuclear Materials

journal homepage: www.elsevier.com/locate/jnucmat

Modelling precipitation in zirconium niobium alloys

J.D. Robson *

Manchester Materials Science Centre, Grosvenor Street, Manchester M1 7HS, United Kingdom

ARTICLE INFO

Article history:
Received 16 January 2008
Accepted 28 March 2008

ABSTRACT

A model has been developed to predict precipitation of β-Nb in zirconium–niobium alloys. The model considers two transformation mechanisms; in situ transformation of any retained β-Zr and homogeneous nucleation of β-Nb. The two mechanisms are allowed to operate concurrently and compete for the available solute. The model has been calibrated and tested using data in the literature and is able to reasonably reproduce these results without introducing non-physical fitting parameters. It has then been applied to predict the effects of prior β-Zr fraction, oxygen content, and temperature on the precipitation kinetics of β-Nb. These calculations predict that prior β-Zr fraction has a strong effect on the kinetics of subsequent β-Nb evolution and that oxygen content is also critical, with higher oxygen levels predicted to result in faster kinetics and shift in the peak transformation rate to higher temperatures.

1. Introduction

Second-phase precipitated particles (SPPs) are critical in controlling the mechanical and corrosion properties of many important engineering alloys. As such, a major effort has been made over several decades to develop models that are capable of predicting important characteristics such as particle volume fraction, size, and distribution as a function of alloy chemistry and processing or service conditions. One aim of such modelling is to gain a better understanding of the effect of these variables on precipitation and guide future alloy and process developments to optimize SPP formation. Another application of SPP modelling is to provide input data to models for property prediction.

Precipitation modelling has tended to focus on widely used alloys where it is known that SPPs play a particularly critical role in determining properties. Thus for steels, age hardenable aluminium alloys, and nickel based superalloys precipitation models have now reached high levels of sophisication. However, there are other alloy systems of great industrial importance where modelling efforts are still in their infancy. An example is modelling the precipitation of SPPs in zirconium based alloys that are widely used in water cooled nuclear power reactors. In a recent paper, Massih and Jernkvist [1] have modelled precipitation in Zircaloy-2 and applied their model to non-isothermal heat treatments as used in industry. However, this is one of the very few examples of application of kinetic modelling to SPP precipitation in zirconium alloys. Latest reactor designs utilize niobium containing alloys, e.g. M5™ [2] (essentially a Zr–1 wt% Nb–O alloy, very similar to the Russian alloy E110), ZIRLO™ [3] (based on the Zr–Nb–Sn–Fe system), and Zr–2.5 wt%Nb–O alloys, used for pressure tube material in Canadian CANDU reactors [4]. Niobium containing SPPs form in these alloys, playing a key role in controlling corrosion resistance, hydriding properties, and grain size evolution (e.g. [5–8]).

To understand the behaviour of the commercial alloys, it is first necessary to understand the behaviour of the binary Zr–Nb system on which they are based. In this work, a model has been developed to predict the precipitation kinetics of β-Nb in binary Zr–Nb alloys. Because of the commercial importance of alloys based on the Zr–Nb system, there have been a number of studies of precipitation (particularly in Zr–2.5 wt% Nb alloys developed for the CANDU reactor programme) that provide data for model calibration and testing. However, there are a number of complicating factors that mean that not all of the data reported in the literature can be used in model validation. Firstly, in some studies under conditions of low Nb supersaturation, there is evidence to suggest that precipitation of metastable β-Zr phase (containing 20 at.% Nb) rather than the equilibrium β-Nb occurs [9]. Secondly, often β heat treatment and quenching conditions are such that β-Zr is retained after cooling from the β phase field [10]. This must be accounted for in a complete model, but such a model can only be tested against experimental data for which the retained β fraction is known, and this is not reported in many studies. Finally, dissolved oxygen is known to have a significant effect on the position of the β phase solvus position [11]. Oxygen concentration is, therefore, a key parameter in determining precipitation kinetics, but not all studies in the literature report its value.

Two studies in particular provide detailed quantitative information on the precipitation of β-Zr in Zr–2.5 wt% Nb alloys that is useful for model testing. Williams and Gilbert [12] used transmission electron microscopy (TEM) to measure the evolution of β-Nb precipitate size and spacing after heat treatment at 500 °C. No β was retained on quenching in their alloy. Toffolon et al. [10,6,5] have performed a detailed study of precipitation in Zr–Nb alloys at

* Tel.: +44 161 306 3560.
E-mail address: joseph.robson@manchester.ac.uk

0022-3115/$ - see front matter © 2008 Elsevier B.V. All rights reserved.
doi:10.1016/j.jnucmat.2008.03.016

570 °C using TEM, calorimetry and X-ray diffraction. Their data provide measurement of the overall precipitation kinetics and the change in matrix niobium level during precipitation. Due to the use of a reduced cooling rate, some β-Zr was retained in the initial microstructure prior to precipitation heat treatment.

There are two potential mechanisms by which β-Nb may form during heat treatment. The first is by classical nucleation and growth of new β-Nb directly from supersaturated α. This occurs when the alloy is rapidly quenched from the single phase β field to form α-martensite, supersaturated in niobium. In alloys with no retained β prior to precipitation heat treatment, direct nucleation and growth of β-Nb is observed [12,13].

The second occurs in alloys which are cooled at slow or intermediate rates from the single phase β field. In this case, retained β-Zr in present after cooling along grain boundaries. This phase is metastable, and on heat treatment the free energy of the system can be reduced by transformation to α and β-Nb. However, this process is complex and can involve intermediate steps, discussed below. Furthermore, the kinetics of the transformation can be extremely slow, taking over 1000 h at 500 °C [14].

The transformation of retained β-Zr below about 530 °C involves an intermediate step in which a metastable hexagonal phase, ω [15], is observed along with β enriched in niobium, but still below the equilibrium concentration. The metastable ω then transforms to α and enriched β-Zr (but this can be very sluggish) and finally to the equilibrium mixture of α + β-Nb [14,4]. Above 530 °C transformation proceeds in the same way but without formation of the intermediate ω phase [14]. Precipitation of ω is observed to accelerate the transformation compared to that expected from extrapolation of the kinetics C-curve measured for conditions where ω does not form [14]. It is important to note that these transformations in the β-Zr phase occur even if the alloy composition is such that the initial condition is 100% β-Zr [14]. The situation will be further complicated when the metastable β-Zr is itself in a matrix of supersaturated α, as occurs for commercial alloy compositions. In this case, diffusion of Nb from the supersaturated α to the β-Zr will also drive the transformation to β-Nb.

In practice, both in situ transformation and nucleation and growth of new β-Nb particles can occur simultaneously. The model developed in this paper allows both mechanisms to occur concurrently, competing for the available solute. The modelling approach for nucleation, growth, and coarsening of new precipitates is based on the Kampmann and Wagner numerical (KWN) method [16]. This is a numerical extension of the analytical Langer Schwartz (LS) model [17], which was used by Massih and Jernkvist [1]. However, the KWN method has been widely used in precipitation modelling in other alloy systems (e.g. [18,19]). To model the in situ transformation of β-Zr a simple diffusion model due to Senior [20] has been used, following Toffolon et al. [10]. Coupling the two models together to predict kinetics in a system where an in situ transformation process can occur concomitantly with classical nucleation and growth, is a key innovation in this work.

Finally, it should be noted that this paper only considers thermal effects and the precipitation of β-Nb as a result of supersaturated Nb retained on quenching. For application to in-reactor performance, the effect of irradiation must also be considered. This can have a very significant effect on the kinetics of the sluggish precipitation kinetics in these alloys, particularly at low supersaturations.

2. The model

2.1. Thermodynamics

To produce a reliable kinetic model, it is first necessary to have a sufficient understanding of the phase equilibria of the system being modelled. Quantities such as equilibrium solubilities and driving forces must be predicted and used as inputs to the kinetic model. Recently, the Calphad approach [21] has been used to assess and model thermodynamic data for the Zr–Nb–O ternary system [11]. This provides data on the equilibrium solubility of Nb in α-Zr as a function of oxygen content that matches well with the experimentally determined phase diagram [22], and is used to calculate the solvus composition in this work.

2.2. In situ transformation of β-Zr

In situ transformation of β-Zr to β-Nb will occur by two mechanisms, which will both be operational simultaneously:

(1) Decomposition of the β-Zr to α + β-Nb, possibly via the formation of an intermediate ω phase, depending on conditions.
(2) Diffusion of Nb from the supersaturated matrix to the β-Zr to provide additional niobium to drive the transformation from β-Zr to β-Nb.

It should be noted that the first mechanism operating in isolation will lead to a net *reduction* in the β fraction as the transformation product (β-Nb) has a much higher niobium concentration. It is useful to consider the effect of the retained β-Zr fraction on the maximum possible fraction of β-Nb that is possible by the two routes identified above. This can be done with a simple Lever Rule calculation from the known equilibrium compositions of the α and β-Nb phases, and the assumption that the β-Zr phase initially contains 20 at.% Nb. Fig. 1 shows the results of such a calculation for a Zr–2.5 wt%Nb alloy. The *x*-axis of this plot shows the amount of niobium remaining in the α phase; when there is no β-Zr clearly all of the niobium is retained in the α. The contribution that mechanism 1 alone could make to the total β-Nb fraction increases as the β-Zr fraction increases, but is only predicted to be dominant once the β-Zr fraction is above approximately 6%, and the niobium remaining in the matrix is less than approximately 1.3 wt% (i.e. roughly half the total niobium content).

In the test case used for the current model, Toffolon et al. [10] determined that the initial matrix composition contained 1.5 at.% niobium, for which case the greatest potential contribution to the increase in β-Nb fraction results from niobium leaving the supersaturated α matrix (mechanism 2). The present model follows Toffolon et al. [10] and assumes that mechanism 2 is dominant. Providing the retained β-Zr fraction is modest (less than about

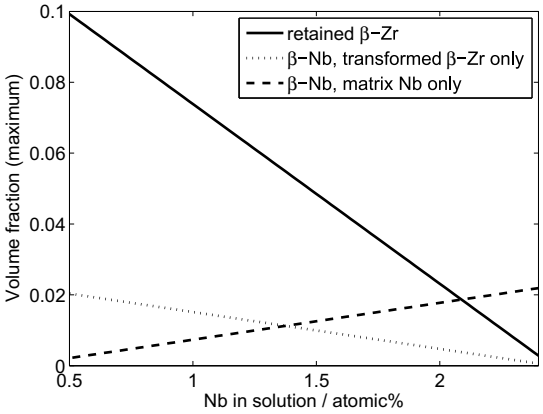

Fig. 1. Retained β-Zr fraction as a function of niobium remaining in the α matrix, used to calculate the maximum possible fraction of β-Nb from transformation of prior β-Zr alone, and the fraction from precipitation of supersaturated Nb present in α.

5% in a Zr–2.5 wt% Nb alloy), Fig. 1 suggests this will be reasonable. This is usually expected to be the case for typical cooling rates used in industrial processing [10]. However, the model will become increasingly inaccurate as the retained β-Zr fraction increases above this value as it ignores the in situ transformation of β-Zr that will occur independently of inward diffusion of niobium (mechanism 1). To include this transformation mode would first requires a better understanding of the composition and thermodynamic properties of the intermediate ω phase.

The model for in situ transformation is based on a simple 1-dimensional model for diffusion of niobium from the matrix to lath boundaries (where the retained β-Zr is situated) that has already been applied by Toffolon et al. [10] to predict solute depletion in the matrix in Zr–2.5 wt%Nb. This model, originally developed for Laves phase precipitation in steel [20], states that in a time step of duration Δt the change in solute concentration at the centre of a lath of width $2L$ is given by [20]:

$$\Delta c_i = \frac{D}{L^2}(c_i - c_e^\alpha)\Delta t, \tag{1}$$

where c_i is the instantaneous concentration of solute Nb in the matrix and c_e^α is the equilibrium concentration of solute in the matrix (α). In reality the solute concentration varies across each lath. However, the KWN framework used for the precipitation model relies on the mean field method to determine the change in matrix composition. It is, therefore, necessary to also use a simplifying mean field approximation in the in situ transformation model to calculate the evolution of the α phase composition. As a first approximation, the depletion in solute concentration is calculated at the lath centre (Eq. (1)) and this change in concentration is assumed to occur across the lath. This is also the approach taken by Toffolon et al. [10]. The requirement for conservation of solute gives a relationship between solute removed from the matrix and the fraction of β-Zr transformed to β-Nb. This is shown graphically in Fig. 2. It is assumed that when niobium diffuses to β-Zr, it causes transformation of a slice of β-Zr to β-Nb. Further niobium diffusion causes the inward growth of this β-Nb, consuming the remaining β-Zr. Balancing the solute removed from the matrix with that taken up by growth of β-Nb gives the increment in volume fraction of β-Nb due as:

$$\Delta V^{\beta Nb} = \frac{\Delta c_i V^\alpha}{(c^{\beta Nb} - c^{\beta Zr})}, \tag{2}$$

where V^α is the volume fraction of the supersaturated α, $c^{\beta Nb}$ is the Nb concentration in β-Nb, and $c^{\beta Zr}$ is the Nb concentration in β-Zr. Fig. 2 also shows graphically the origins of this equation, since for conservation of solute, the two shaded regions must have the same area.

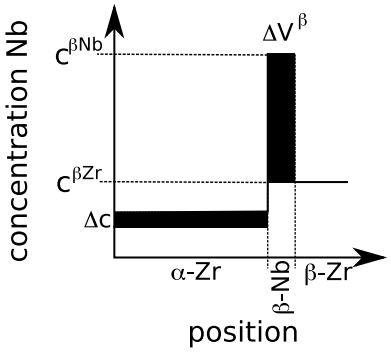

Fig. 2. Schematic showing how the solute removed from the matrix relates to the fraction of β-Zr transformed to β-Nb. For conservation of solute, the two shaded areas must be equal. All terms are defined in the text.

2.3. Nucleation of new precipitates

The equilibrium solvus composition can be used to calculate the driving force for nucleation of new β-Nb precipitates [23]

$$\Delta G_v = -\frac{R_g T}{V_a}\left[c^{\beta Nb}\frac{\ln(c_i)}{\ln(c_e^\alpha)} + (1 - c^{\beta Nb})\frac{\ln(1-c_i)}{\ln(1-c_e^\alpha)}\right], \tag{3}$$

where V_a is the molar volume of the precipitating phase.

To model growth and coarsening, it is necessary to account for the effect of capillarity on the equilibrium composition at the particle/matrix interface. The concentration of solute in the matrix in equilibrium with a particle of radius r may be calculated from c_∞^α (the equilibrium concentration of solute in the matrix for a planar interface) using the Gibbs–Thomson equation:

$$c_r^\alpha = c_e^\alpha \exp\left(\frac{2\sigma V_m}{R_g T}\frac{1}{r}\right), \tag{4}$$

where c_r^α is curvature compensated matrix composition at the interface for a particle of radius r, σ is the interfacial energy, V_m the molar volume of the product phase and R_g and T have their usual meanings.

In the KWN method, the classical theory of nucleation is used to model the time dependent nucleation rate. Classical nucleation theory gives the equation for homogeneous nucleation as [16,24]

$$I = N_v Z \beta^* \exp\left[\frac{-4\pi\gamma r^{*2}}{3kT}\right]\exp\left(-\frac{\tau}{t}\right), \tag{5}$$

where N_v is the number of nucleation sites per unit volume (equal to the number of atoms per unit volume for homogeneous nucleation), Z is the Zeldovich factor (which accounts for the decay of some of the supercritical clusters), γ is the interfacial energy of the nucleus (which is assumed to be isotropic and size independent), r^* is the critical radius a cluster must reach to become a nucleus and τ is the incubation time for nucleation (the time taken to establish the initial cluster distribution). k and T have their usual meanings.

The critical radius depends on the driving force for transformation and the interfacial energy. Ignoring strain energy, the critical radius may be written as:

$$r^* = \frac{-2\gamma}{\Delta G_v}, \tag{6}$$

where ΔG_v is given by Eq. (3).

Using the assumption of a spherical nucleus, the Z, β^* and τ values may be written [24–26].

$$Z = \frac{V_\alpha \Delta G_v^2}{8\pi\sqrt{\gamma^3 kT}}, \tag{7}$$

$$\beta^* = \frac{16\pi\gamma^2 c_i D}{\Delta G_v^2 a^4}, \tag{8}$$

$$\tau = \frac{8kT\gamma a^4}{V_\alpha^2 \Delta G_v^2 Dc}, \tag{9}$$

where V_α is the volume per atom in the matrix, a is the lattice constant of the product phase and D is the diffusivity of the solute in the matrix, which is calculated in the usual way [27]. For the diffusion of Nb in α-Zr the data of Dyment and Libanati [28] were used.

Experimentally, both homogeneous nucleation of β-Nb within the matrix and heterogeneous nucleation (e.g. on lath boundaries) have been observed. The present model deals explicitly with homogeneous nucleation of β-Nb within grains, and heterogeneous formation by transformation of prior β-Zr on lath boundaries. The development and calibration of separate model for heterogenous nucleation of β-Nb requires more detailed quantitative experimental information about this precipitation mode which is not yet

available. The limitations of this omission from the model will be discussed in the results section.

Williams and Gilbert [12] report the evolution of particle size and spacing of homogeneously nucleated particles and this data was used to calibrate the present model. For homogeneous nucleation, the only unknown parameter in the kinetic equations is the interfacial energy of the nucleating phase. This was adjusted until the predicted precipitate size and spacing agreed best with that measured experimentally [12]. Once fixed, this parameter is expected to be largely independent of changes in temperature and thus the model can be used to make predictions for different conditions, including non-isothermal treatments.

2.4. Growth and coarsening

To a first approximation, it was assumed that β-Nb particles grow with an approximately spherical morphology at a rate controlled by bulk diffusion of Nb in α-Zr (the predictions are not particularly sensitive to the choice of particle shape). The diffusion controlled growth rate is given by [29]:

$$\frac{dr}{dt} = \frac{D}{r}\frac{c_i - c_r^\alpha}{c^{\beta Nb} - c_r^\alpha}, \tag{10}$$

where c_r^α is calculated from the equilibrium concentration of solute in the matrix for a planar interface using the Gibbs–Thomson equation (4).

Coarsening occurs when large precipitates grow at the expense of small ones, without a change the overall volume fraction. This process, driven by a reduction in the overall interfacial energy, arises naturally in the KWN model. As the fraction of solute in the matrix decreases during precipitation, the driving force for nucleation and growth of the precipitate particles decreases and the critical particle radius increases. Particles in the size distribution which have a radius $< r^*$ will have a negative growth rate according to Eq. (10) and will thus start to shrink. Particles with a radius $> r^*$ will retain a positive growth rate and will continue to increase in size. When the size of a group of shrinking particles reaches zero they are removed from the size distribution.

2.5. Kinetics model

The equations for nucleation and growth are coupled using Kampmann and Wagner Numerical (KWN) model, which has been described in detail elsewhere [16,19,30]. In this work, the nucleation and growth model is run concomitantly with the in situ transformation model (for cases where prior β-Zr is present). The two sub-models are linked together through the competition for available solute. The essential features of the computational implementation of the model are summarized below:

(1) The continuous time evolution of the particle distribution and matrix chemistry is considered in terms of discreet time steps.
(2) The continuous size distribution of particles formed by nucleation and growth is discretized into a large number of size classes.
(3) The number of new particles in each time step is calculated using classical nucleation theory. The exchange of particles between size classes is calculated assuming solute diffusion is the rate limiting process and a spherical growth morphology. The Gibbs Thomson relationship is used to calculate the modified interfacial compositions for each size class and at each time step.
(4) The change in matrix solute level due to (i) precipitate nucleation and growth, (ii) precipitate dissolution, and (iii) transformation of prior β-Zr is calculated at each time step using the mean field approximation.
(5) The volume fraction of β-Nb is calculated by adding up the contribution from independently nucleated particles and transformed β-Zr.

The resultant model is capable of predicting nucleation, growth, coarsening, and in situ transformation without artificial constraints, whether these processes occur concommitantly or sequentially. The model developed here uses a Runge–Kutta scheme to determine the time interval for each step to ensure model efficiency and numerical accuracy, and this is discussed in detail elsewhere [31].

3. Results

3.1. Model calibration

The model was calibrated using two data-sets in the literature that provide detailed information on the evolution of β-Zr precipitates in Zr–2.5 wt% Nb alloys for two temperatures and initial conditions. Williams and Gilbert [12] performed a transmission electron microscopy (TEM) study of precipitation at 500 °C in β quenched material and measured the evolution of mean precipitate diameter and spacing. Their measurements explicitly differentiate between homogeneous precipitates formed in the matrix and heterogeneous precipitates nucleated on twin and lath boundaries.

Toffolon et al. [10,6,5] performed heat treatments at 570 °C on material that contained retained β after cooling and measured the evolution of niobium in the matrix and β-Nb volume fraction by calorimetry [10,6]. The initial condition of their alloy was such that the measured initial niobium concentration in the matrix was 1.5 at.%, due to the presence of β-Zr. In both studies, the oxygen level reported in the alloys were similar (1400 ppm [12] and 1200 ppm [6]) and the model accounts for the (small) effect of this difference on the solubility of niobium.

There are two calibration parameters in the model; the interfacial energy of the β-Nb phase for nucleation and growth and the lath width 2*L* for in situ transformation. The lath width was determined by reproducing the model results of Toffolon et al. [10] using the in situ transformation model only (turning off the nucleation and growth model). Since the same model was used, this gave a perfect match. The interfacial energy was calibrated using the Williams and Gilbert data-set [12], as already described.

Fig. 3 shows a comparison of the predicted and measured particle size and spacing for the best fit value of the interfacial energy. It can be seen that for times less than about 20 h the predicted particle size and spacing agrees well with experiment. Note that the particle spacing is predicted to first decrease (as new nuclei form), plateau (as nucleation saturates), and then increase (as coarsening becomes significant and small particles dissolve). The particle spacing during the early stages is determined principally by the nucleation rate, and the good agreement between prediction and measurement suggests that the calculation of nucleation rate is reasonably accurate.

However, at longer times, the model predictions increasingly deviate from the measurements. This is during a regime where the model predicts that precipitate evolution is dominated by coarsening. Experimentally, this coarsening was also observed, but it took place predominantly by growth of the precipitates formed at heterogeneous sites, which were excluded from the experimental data-set used to determine the particle size for homogeneous particles. The model, however, does not explicitly track these two precipitate populations. Therefore, an increase in the average particle size as predicted by the model at times over 20 h is observed in reality, but is caused by preferential coarsening of the heterogeneous precipitates and so is not reflected in the

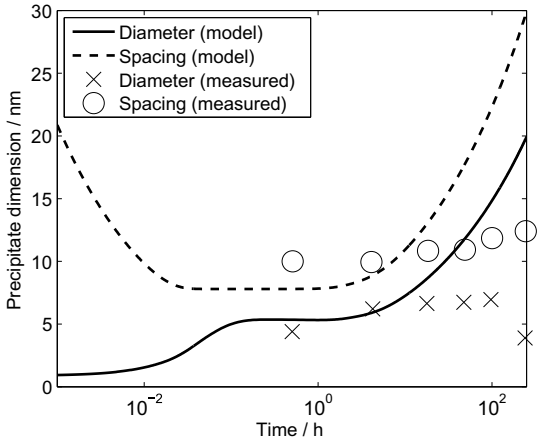

Fig. 3. Predicted evolution of precipitate size and spacing at 500 °C compared with the measured data for homogeneous precipitates from Williams and Gilbert [12].

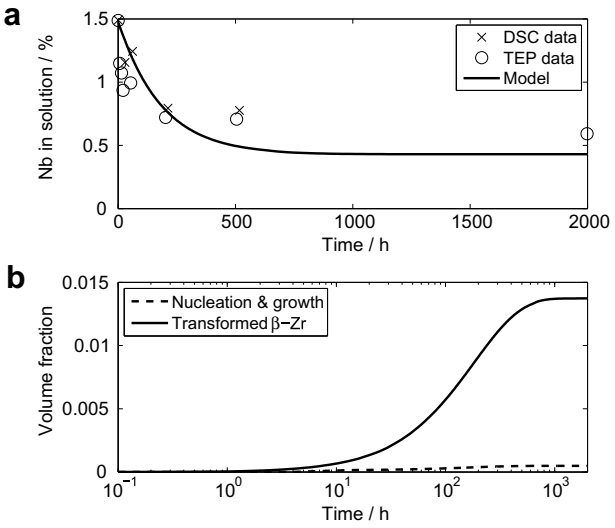

Fig. 4. Predicted evolution of (a) matrix niobium level and (b) volume fraction of β-Nb at 570 °C. The experimental data in (a) are from the differential scanning calorimetry (DSC) and themo-electric power (TEP) measurements of Toffolon et al. [6,10].

measurements for homogeneous particles. A more complex model would be needed to account explicitly for the two precipitate populations. This is not yet justified given current limitations in experimental data and understanding of the precipitation process.

The final set of input parameters to the model are shown in Table 1. Confidence in the model is increased by noting that the best fit parameters have values that fall within the range that would be expected for the physical values to which they relate. For example, an interfacial energy of 0.25 J m^{-2} is physically reasonable and is the same as that used for modelling nucleation of other cubic phases in zirconium alloys [1].

The coupled model (including both transformation of existing β-Zr and formation of new precipitates) was then applied to the predict precipitation under the conditions studied by Toffolon et al. [10]. Fig. 4 shows the predicted evolution of matrix niobium level (a) and volume fraction of β-Nb (b) formed by both in situ transformation and nucleation/growth. It can be seen that in this case, the model predicts that in situ transformation dominates, and the volume fraction formed by independent nucleation and growth is expected to be very small. The depletion of niobium in the matrix is, therefore, dominated by diffusion of niobium to the lath boundaries, as assumed by Toffolon et al. [10], and the model successfully reproduces the change in matrix chemistry.

3.2. Effect of prior β-Zr

With the present model it is possible to go further and investigate the effect of the prior β-Zr fraction on subsequent precipitation of β-Nb. It has already been shown that at 570 °C for the case of a Zr–2.5 wt% Nb alloy, where the β-Zr fraction is sufficient to reduce the matrix composition to 1.5 at.%, in situ transformation is predicted to dominate. Calculations were performed for the same alloy and conditions, but assuming an initial matrix composition of 2.5, 2, and 1.75 at.% Nb, with the remainder tied up in β-Zr.

Table 1
Model input parameters

Parameter	Value
Nucleation site density $N_{effective}$	1.29×10^{21} m^{-3}
Lath width $2L$	3.5 μm
Effective interfacial energy $\gamma_{effective}$	0.19 J m^{-2}
Activation energy for diffusion Q	131 kJ mol^{-1}
Pre-exponential for diffusion D_0	6.6×10^{-10} m^2 s^{-1}

Diffusion data from Dyment and Libanati [28].

For these compositions, the initial β-Zr fraction can be seen by reference to Fig. 1 and in all cases the dominant in situ transformation mechanism is expected to be due to diffusion of supersaturated Nb from the α. The predicted volume fraction evolution in each case is shown in Fig. 5.

It can be seen that for all initial matrix compositions in the range 1.75–2.5 at.% Nb, nucleation and growth is predicted to dominate the overall transformation kinetics. The rate of precipitation reduces as the initial supersaturation in the matrix falls. The in situ transformation mode is slow, since the diffusion distances are greater than for homogeneous nucleation/growth, and the diffusion rate of niobium in zirconium is very slow. For an initial matrix composition of 2 at.% Zr, it is predicted that nucleation and growth is essentially complete before significant in situ transformation occurs. It is interesting to note in this case that the volume fraction of precipitates formed by nucleation and growth is predicted to decrease as the in situ transformed fraction increases. This is because the reduction in matrix supersaturation due to diffusion of niobium to the lath boundaries destabilizes the finest homogenous precipitates, which dissolve.

An initial matrix composition of 1.75 at.% Zr results in a situation where nucleation and growth occur together during the early stages of transformation. It should be noted that in all cases where prior β-Zr exists, complete transformation to β-Nb had not occurred by the end of the simulation run. Only when the initial matrix composition was reduced to 1.5 at.% Nb did in situ transformation dominate the overall kinetics, as already discussed.

Although these calculations are untested, the predicted effect of a change in retained β-Zr fraction on subsequent β-Nb evolution is reasonable, and demonstrates that changing the retained β-Zr fraction will have a strong influence on subsequent SPP formation (including the size and spacing as well as volume fraction of SPPs, which are also predicted by the model but not shown here for brevity). The model also suggests that a transition from nucleation and growth to in situ dominated kinetics will occur and for a given alloy this is sensitive to small changes in the initial matrix solute level.

3.3. Effect of oxygen content

Oxygen is known to have a significant influence on the solubility of niobium in α-Zr and, therefore, a change in oxygen content

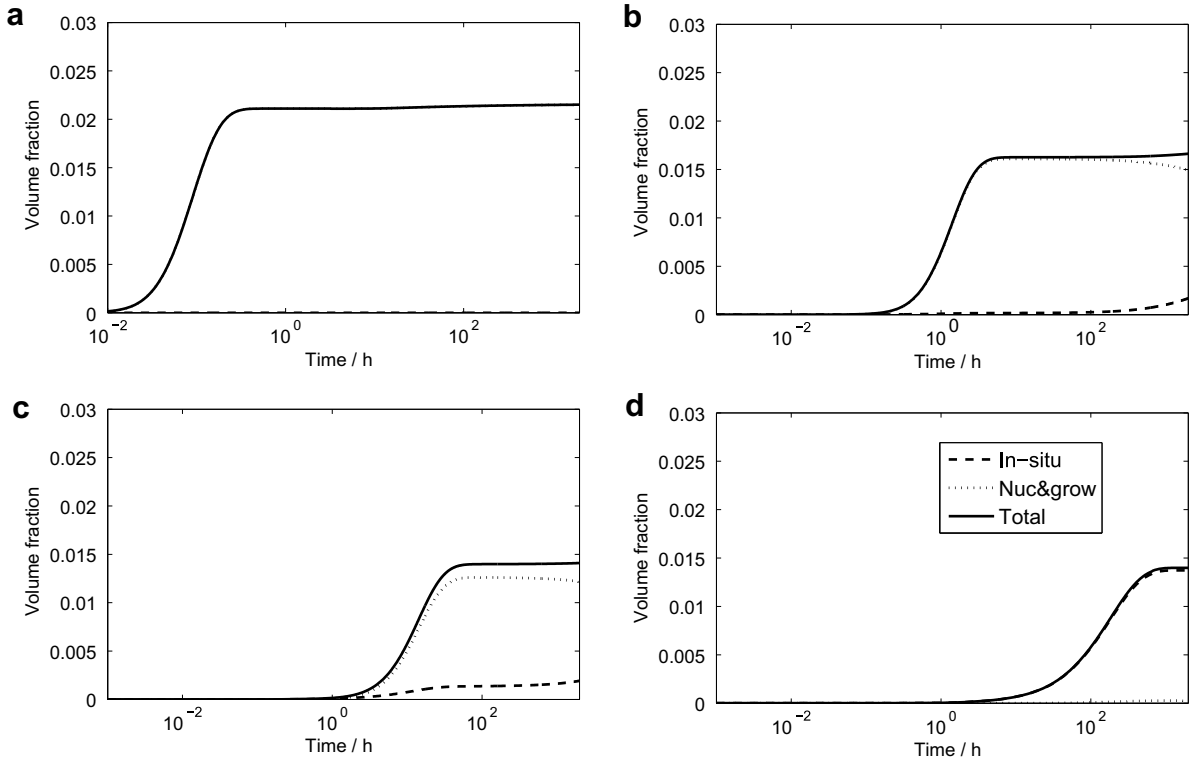

Fig. 5. Prediction of the evolution of volume fraction of β-Nb in Zr–2.5 wt% Nb at 570 °C with different initial matrix compositions (at.%) and retained β-Zr fractions. The volume fraction contributions from in situ transformation of β-Zr and nucleation/growth are also shown. Initial matrix composition (a) 2.5, (b) 2, (c) 1.75, and (d) 1.5 at.%.

will change the supersaturation of niobium and the precipitation kinetics. The model was used to investigate the effect of oxygen content on the overall precipitation kinetics of β-Nb in Zr–2.5 wt% Nb (assuming no retained β-Zr). The assumption of no retained β greatly simplifies the calculation, since only the direct precipitation of β-Nb need be considered. Thus, complexities in the shape of the time–temperature-transformation behaviour which are seen for the in situ transformation of β-Zr [14], and are due to the transition phases, are avoided.

The predicted overall kinetics are plotted in the form of a time–temperature-transformation (TTT) diagram in Fig. 6, showing the predicted time to reach a precipitate volume fraction of 1%. As the oxygen content is increased from 300 to 1500 ppm, the time taken to precipitate 1% β-Nb is predicted to decrease sharply, and the nose in the TTT curve moves to a higher temperature. This is due to an increase in niobium supersaturation as oxygen level is increased. The TTT diagram also shows that it is predicted that precipitation occurs most rapidly between about 520 and 540 °C depending on the oxygen concentration.

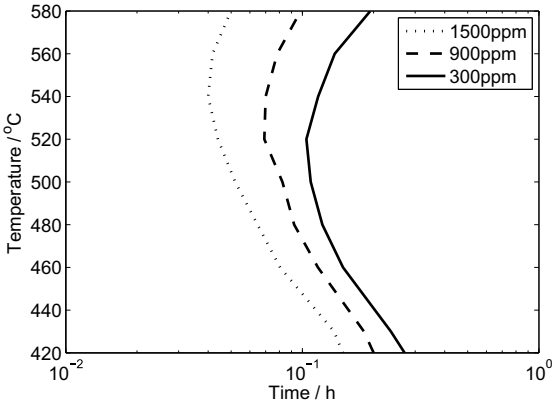

Fig. 6. Time–temperature-transformation diagram. Curves are plotted corresponding to the precipitation of 1% β-Nb in a Zr–2.5 wt% Nb alloy for three oxygen levels; 300, 900, and 1500 ppm.

3.4. Precipitation at lower temperature

The model testing and calibration has been carried out in the temperature range 500–570 °C, as this is the range for which data were available in the literature. However, for in reactor performance, the temperature range 250–360 °C is of more interest. One of the problems in studying precipitation experimentally is that in the absence of radiation, the kinetics of β-Nb formation at these temperatures are known to be very sluggish. The model was applied to predict the expected precipitation kinetics between 250 and 350 °C for a Zr–2.5 wt% Nb alloy with 1400 ppm oxygen, assuming no β-Zr is retained on quenching. A plot of the predicted volume fraction of β-Nb with time is shown in Fig. 7. Since the predictions in this temperature range are far below the model calibration temperature, and there is also greater uncertainty in the phase boundary positions, these calculations are likely to be subject to considerable error. Nevertheless, they demonstrate that between 250 and 350 °C, β-Nb precipitation is indeed predicted to be very slow. For example, at 250 °C, it is predicted to take over 100 years to reach the equilibrium β-Nb fraction in the absence of irradiation. An increase in temperature by 100–350 °C, has a marked accelerating effect on the predicted precipitation kinetics, reducing the time to reach the equilibrium β-Nb fraction to approximately 1 week. It is important to note that at these low temperatures, the atomic displacements produced by irradiation will have a strong effect on the movement of niobium, and therefore on the precipitation kinetics of β-Nb. A complete model for in-reactor SPP evolution would, therefore, need to ultimately include these effects.

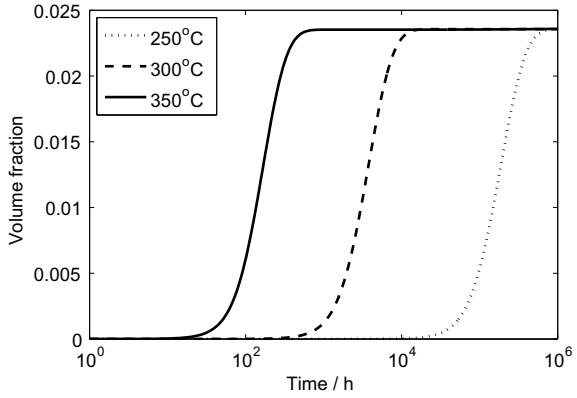

Fig. 7. Predicted evolution of β-Nb volume fraction as a function of time in a Zr–2.5 wt% Nb alloy at 250, 300 and 350 °C.

3.5. Evolution of particle size, number, and size distribution

One of the advantages of the KWN model is that it gives full details of the evolution of the particle size distribution throughout precipitation. From this information, averaged precipitate parameters such as mean particle size can be extracted. Fig. 8 shows the predicted evolution of mean particle size and number density for Zr–2.5 wt% Nb at three temperatures (assuming no retained β-Zr). The number density evolution shows the expected shape for a precipitation and coarsening process. The initial increase in number density is due to nucleation of new particles. The nucleation rate then falls sharply as the matrix supersaturation is reduced, and there is a plateau in the number density. Finally, the smallest particles start to dissolve under the influence of coarsening and the particle number density starts falling. It is predicted that for precipitation at 420 °C the particle size in the early stages (prior to the transition to coarsening dominated kinetics) is very small, with a mean particle radius of only 2 nm. For this temperature, particles are only likely to be easily observed in the TEM once coarsening has become established. The model results also suggest that in many studies of β-Nb precipitation, where the microstructure is evaluated after several hundred hours [10], the observed particles will have undergone extensive coarsening.

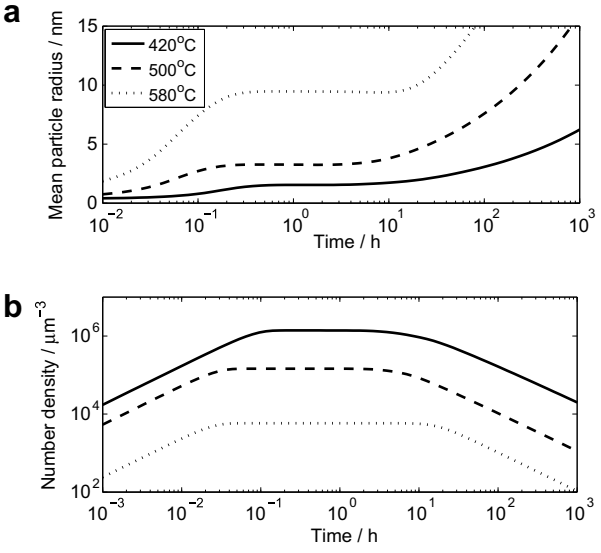

Fig. 8. (a) Predicted evolution of mean particle size in Zr–2.5 wt% Nb at three precipitation temperatures. (b) Predicted number density evolution for the same conditions.

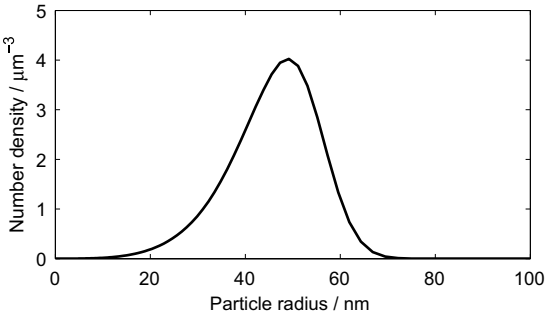

Fig. 9. Predicted particle size distribution for β-Nb particles after 1000 h at 580 °C (Zr–2.5 wt%Nb alloy).

After long times at elevated temperatures (e.g. 1000 h at 580 °C) the predicted particle size distribution (PSD) tends towards a steady state shape (Fig. 9). This is similar to the distribution expected from Lifshitz–Slyozov–Wagner (LSW) coarsening theory [32,33], but slightly broader. Such size distributions are typically observed experimentally after extensive coarsening, and this aspect of the KWN model is discussed in detail elsewhere [34].

4. Conclusions

A model has been developed to predict β-Nb precipitation in Zr–Nb alloys. The model considers two transformation modes; in situ transformation of retained β-Zr (if present) and nucleation, growth, and coarsening of new β-Nb particles. The model has been calibrated using the limited data available in the literature, and applied to make a number of predictions for Zr–2.5 wt% Nb alloys, the conclusions from which are summarized below.

(1) There is a competition for solute between in situ transformation and new particles. The fraction of retained β-Zr, therefore, has a strong effect on the volume fraction and precipitation kinetics of new β-Nb particles.
(2) The transition from transformation dominated by in situ transformation to transformation dominated by nucleation and growth is predicted to occur sharply as the fraction of retained β-Zr is reduced.
(3) Oxygen content is predicted to have a strong effect on precipitation kinetics, with an increased oxygen level both accelerating precipitation and shifting the nose of the predicted TTT-diagram to higher temperatures.
(4) In Zr–2.5 wt% Nb with no retained β-Zr the most rapid precipitation kinetics are predicted to occur between ≃520 and 540 °C, depending on oxygen content.
(5) Prediction of the evolution of particle size and number density suggest that for many experimental studies, coarsening is well established at the point that observations of precipitation are made. Prior to this, at relatively low temperatures (e.g. 420 °C), a very fine particle distribution is predicted to form.
(6) Application of the model to temperatures typical of reactor service (250–350 °C) suggest that in the absence of radiation effects, the precipitation kinetics are very sluggish. For example in a Zr–2.5 wt% Nb alloy it is predicted to take over 100 years to reach the equilibrium fraction of β-Nb at 250 °C.
(7) The predicted particle size distribution at long times shows tends to a slightly broadened LSW distribution as expected.
(8) Modelling enables many parameters that are difficult to measure experimentally to be tracked continuously, providing insights into the precipitation process. Validation is critical to this, and current efforts are focussed on generating

additional experimental data to test and refine the model presented here as well as applying it to the complex thermal paths used in industry.

(9) For practical application to in-reactor behaviour, the effect of irradiation on kinetics need to be accounted for in the model, and this represents a major challenge.

Acknowledgements

The author is grateful to Dr Michael Preuss and Maria Ivermark of the Manchester School of Materials for valuable discussions regarding this work. Maria Ivermark is thanked for her translation of Ref. [10].

References

[1] A.R. Massih, L.O. Jernkvist, Comput. Mater. Sci. 39 (2007) 349.
[2] J.P. Mardon, G. Garner, P. Beslu, D. Charquet, J. Senevat, in: Proceedings of the 1997 International Topic Meeting on LWR Fuel Performance, Portland, Oregon, 2–6 March, 1997, p. 405.
[3] G.P. Sabol, G.R. Kilp, M.G. Balfour, E. Roberts, ASTM STP 1023 (1989) 227.
[4] S.A. Aldridge, B.A. Cheadle, J. Nucl. Mater. 42 (1972) 32.
[5] C. Toffolon-Masclet, T. Guilbert, J.C. Brachet, J. Nucl. Mater. 372 (2008) 367.
[6] C. Toffolon-Masclet, P. Barberis, J.C. Brachet, J.P. Mardon, L. Legras, J. ASTM Int. STP 1467 (2) (2005) 81.
[7] Y.H. Jeong, H.G. Kim, T.H. Kim, J. Nucl. Mater. 317 (2003) 1.
[8] P. Barberis, D. Charquet, V. Rebeyrolle, J. Nucl. Mater. 326 (2004) 163.
[9] S. Banerjee, S.J. Vijayakar, R. Krishnan, J. Nucl. Mater. 62 (1976) 229.
[10] C. Toffolon, J.C. Brachet, T. Guilbert, D. Hamon, S. Urvoy, C. Servant, D. Charquet, L. Legras, J.P. Mardon, J. Phys. IV France 11 (2001) 99.
[11] R. Jerlerud Pérez, A.R. Massih, J. Nucl. Mater. 360 (2007) 242.
[12] C.D. Williams, R.W. Gilbert, J. Nucl. Mater. 18 (1966) 161.
[13] G.P. Sabol, J. Nucl. Mater. 34 (1970) 142.
[14] B.A. Cheadle, S.A. Aldridge, J. Nucl. Mater. 47 (1973) 255.
[15] B.A. Hatt, J.A. Roberts, Acta Metall. 8 (1960) 575.
[16] R. Kampmann, R. Wagner, Materials Science and Technology, vol. 5, VCH Weinheim, Germany, 1991.
[17] J.S. Langer, A.J. Schwartz, Phys. Rev. A A21 (1980) 948.
[18] J.D. Robson, Acta Mater. 52 (2004) 1409.
[19] O.R. Myhr, Ø. Grong, Acta Mater. 48 (2000) 1605.
[20] B.A. Senior, Mater. Sci. Eng. A A119 (1989) L5.
[21] N. Saunders, P. Miodownik, Calphad – Calculation of Phase Diagrams, Pergamon, London, 1998.
[22] H. Okamoto, J. Phase Equilibria 13 (5) (1992) 557.
[23] H.I. Aaronsonn, C. Laird, K.R. Kinsman, Phase Transformations, American Society of Metals, 1970.
[24] F.K. LeGoues, H.I. Aaronson, Acta Metall. 32 (1984) 1855.
[25] K.C. Russell, in: H.I. Aaronson (Ed.), Phase Transformations, American Society of Metals, Metals Park, OH, 1970, p. 219.
[26] K.C. Russell, Adv. Colloid Interf. Sci. 13 (1980) 205.
[27] J.W. Christian, Theory of Transformations in Metals and Alloys, Part 1, Pergamon, Oxford, 1975.
[28] F. Dyment, C.M. Libanati, J. Mater. Sci. 3 (1968) 349.
[29] H.B. Aaron, D. Fainstain, G.R. Kotler, J. Appl. Phys. 41 (1970) 4404.
[30] J.D. Robson, P.B. Prangnell, Acta Mater. 49 (2001) 599.
[31] J.D. Robson, M.J. Jones, P.B. Prangnell, Acta Mater. 51 (2003) 1453.
[32] I.M. Lifshitz, V.V. Slyozov, J. Phys. Chem. Solids 19 (1961) 35.
[33] C. Wagner, Z. Electrochem. 65 (1961) 581.
[34] J.D. Robson, Mater. Sci. Technol. 20 (2004) 441.